Geosynthetics Asia'97, 26–29 November, Bangalore, India

POORLY DRAINING GEOTEXTILE REINFORCED RETAINING WALLS — A NUMERICAL STUDY

Masaki Kobayashi[1] and Ali Porbaha[2]

[1] Port and Harbour Research Institute, 3-1-1 Nagase, Yokosuka 239, Japan
[2] Technical Research Institute, TOA Corporation, Yokohama, Japan

ABSTRACT: In the light of advances in geosynthetic materials the fabric reinforced walls are getting more cost-effective than the conventional concrete walls in both developed and developing countries. In addition, the use of locally available fill significantly reduces the overall cost of the project. Among many issues related to geosynthetics, the method of analysis of soil retaining structures is still a subject of debate. This study presents the numerical modeling of physical tests on scaled geotextile reinforced retaining walls. The aim is to predict the position of critical slip surface which is an important factor in cost-effective design of retaining systems. The effects of maximum shear strain contours and plastic yield zones on the positions and traces of slip surfaces were investigated for unreinforced and reinforced vertical walls.

1.0 INTRODUCTION

Rapid economic development in many countries of the world has prompted engineers and researchers to search for new materials for cost-effective expansion of infrastructures. The use of fabrics in construction industry, collectively referred to as geosynthetics, is in parallel to these efforts. In the last couple of decades various type of geosynthetics have gained acceptance as reinforcing materials in a variety of soil structures.

This acceptance has evolved rapidly, although geotechnical engineering is an understandably conservative discipline. Partially, it is because of the design tools that have been developed based on sound geotechnical engineering and on proven performance. It is also due to the available variety of properties of this engineered material. Geosynthetics can be made strong under tension, typically ductile, easy to handle and to construct with, and, depending on the type of the polymer, inert and durable in many applications. Consequently, the use of geosynthetics as soil reinforcement is attractive, allowing flexibility in design. The main factor in propagating the use of geosynthetics, however, is its cost-effectiveness. In many cases, use of geosynthetics offers a cost-effective alternative to other conventional solutions (see Figure 1). Several issues, all related (directly or indirectly) to design, still remain debatable. These issues should not infer lack of confidence in using geosynthetics but rather highlight some topics that need further research, clarification, and possibly modification.

In fact, areas in geotechnical engineering that are more established than geosynthetic reinforcement are constantly being modified (e.g., slope stability, deep and shallow foundations, ground water flow). Yet, existing design procedures in these areas are routinely and safely being employed in major projects. The issues in geosynthetic reinforcement should, perhaps, be viewed in a similar context.

Several researchers have applied small scale tests to model geotechnical problems (see, for example, Mitchell et al. ,1988; and Bolton et al., 1978). The literature contains a large number of cases in which finite element analysis was applied for predicting the performance of field or laboratory tests (see, for example, Rowe and Soderman, 1985; Wu et al.,1992).This article presents the numerical simulation of scaled models of geotextile reinforced walls constructed with cohesive backfill, in parallel to the work by Porbaha and Kobayashi (1997) that investigated the behavior of sloping walls of 1H:6V.

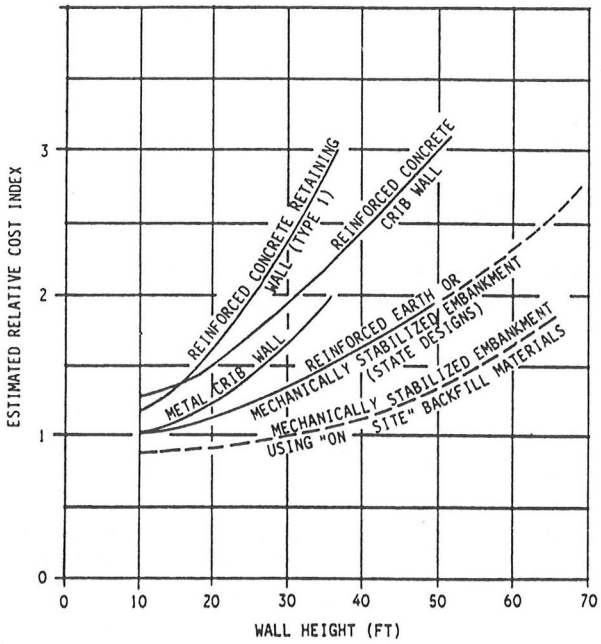

Figure 1: Relative cost comparison of various retaining walls, based on 1974 cost data (provided by California Department of Transportation, reported by Mitchell and Villet, 1987)

2.0 PHYSICAL TESTS

Tests were conducted on reduced scale model walls under an artificial gravity caused by a geotechnical centrifuge. The induced self-weight due to increase in gravitational acceleration develops tension crack that leads to failure. In this study hydrite kaolin was used for the backfill and for the foundation of all models. The liquid limit of the kaolin is 49% and the plastic limit is 33%. The model walls were constructed in a rigid aluminum container with inside dimensions of 400 mm by 300 mm in area, by 300 mm in depth. For these models the foundation was firm in which the soil was mixed at optimum moisture content and then compressed, increasing stress slowly using a single loading plate to reach a maximum vertical stress of 337 kN/m^2. When that stress was reached, the load was immediately removed. This produced a clay foundation with a dry unit weight of 13.5 kN/m^3. The result was a foundation layer that was firmer than the same kaolin prepared for the retained fill and the backfill of the model walls.

After foundation preparation, an aluminum block was laid on the foundation at the toe of the wall to be constructed, to provide lateral support during model construction. The inside vertical side boundaries of the container were sprayed with silicon, and overlain with a thin plastic film to reduce boundary friction effects. The first layer of reinforcement was then placed on the exposed portion of the foundation, a layer of soil placed on it, and the geotextile folded back into the soil to provide a flexible facing for the wall. A compressive stress was then applied increasing slowly to a maximum of 175 kN/m^2. The result was a lift of backfill and retained fill with dry unit weight of 12.3 kN/m^3. This process was repeated for successive layers, each of which had finished thicknesses of 19 mm, until the model wall reached the desired height. A profile of a model is shown in Figure 2. The lateral support blocks were then removed before the centrifuge test. A full height lateral support during construction is not desirable in the field, since it is beneficial to develop gradual tensioning of the reinforcement as a wall is constructed. This gradual tensioning is achieved in the centrifuge models during the steadily increasing self-weight loading. The top of the model was sprayed with dark paint to highlight the development of tension cracks on the surface of the white clay. On the vertical side of the

model, which would be visible during the test through a Plexiglas window. a grid of dots was painted to highlight cross-sectional deformation.

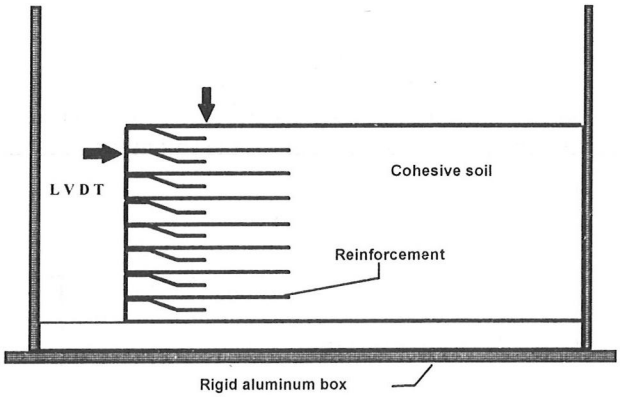

Figure 2: Geometry of a model wall

Models were exposed to an artificial gravity induced by geotechnical centrifuge by increasing gradually the self-weight of the model until failure occurred. The rate of these increases was 2g/minute until cracking was observed, at which point the rate was decreased, allowing any wall movement to cease before further increases were made. After a test, the model was disassembled to examine the deformations of the reinforcements at different elevations. The coordinates of the failure surfaces were recorded using a profilometer, measuring the vertical profile at 10 mm horizontal intervals through various model cross-sections. Direct shear tests were performed on specimens retrieved at various depths in the unfailed rear portion of the model after failure, subjecting each to normal stresses equal to the maximum experienced by the specimen during a test due to overburden load.

Table 1 presents the model geometry of the model tests built on firm foundations. Reinforcement configurations varied from no reinforcement, to a maximum reinforcement length of 114 mm or 0.75 times model wall height, with eight layers of reinforcement in every model. Further discussion on the behaviors of these models in terms of development of tension crack, foundation rigidity, and stability analysis is presented by Porbaha and Goodings (1996).

Table 1. Geometries and properties of model walls

Model No.	Length (mm)	L/H ratio	Cohesion (kN/m^2)	Friction angle (deg.)
M-34	0	0	16.3	21.3
M-48	76	0.50	18.6	20.1
M-49	100	0.66	17.8	21.5
M-28	114	0.75	20.0	20.8

L/H= Length of reinforcement per model height

3.0 FEM ANALYSIS

The program developed by Kobayashi (1984) for the analysis of geotechnical program is used in this investigation to perform numerical simulation of model walls. The two dimensional finite element mesh used for the analysis is shown in Figure 3. The geometry of the mesh is selected to ensure proper modeling of the wall identical to the physical model. The finite element mesh consists of 336 nodes and 141 elements to simulate the backfill, the foundation, and the reinforcement.

Different types of elements are used to model the backfill, the foundation, and the reinforcement. The simulation comprises of eight-noded quadrilateral isoparametric solid elements to model the soil in the backfill and the foundation, and three-noded bar elements for the reinforcement. The six-noded joint

elements is commonly used to simulate the soil-interface interaction and to apply the properties based on the results obtained from laboratory pullout tests. However, the implementation of such a process seems obscure in this study. The reason is that the backfill material is a partially saturated soil and the hydraulic characteristics of nonwoven geotextile allows drainage in both sides of the reinforcement. Accordingly, the moisture content of the soil which tends to be peak value at the center of the soil layer reaches a minimum value at the interface in the vicinity of the reinforcement, and thus creating a complex soil profile that is difficult to model in ordinary pullout tests. For this reason to resolve this issue the interface between soil and geotextile is considered to be the same as the soil model, despite some deficiencies with the complex real situations.

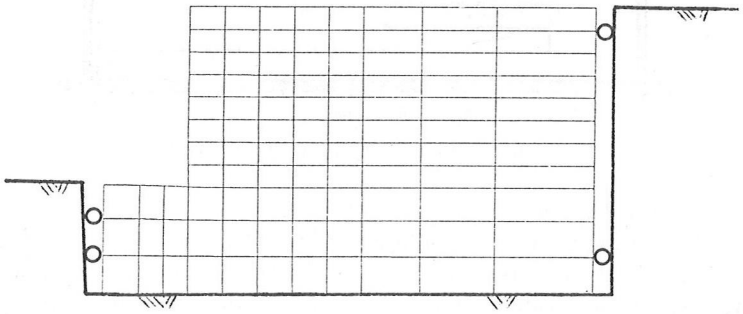

Fig. 3 Finite element mesh and boundary conditions

The constitutive models commonly used to study the behavior of reinforced retaining structures at failure are based on Mohr-Coulomb yield criterion. The elasto-plastic soil properties based on Mohr-Coulomb failure criterion were derived from laboratory tests for each model slope, as listed in Table 1. Poisson ratio of 0.30 was adopted for the analysis. The reinforcement was modeled as beam element with axial stiffness of 0.1 kN/m and no flexural rigidity (due to the extensibility of the reinforcement). The tensile strength of the geotextile from zero-span laboratory test was 0.117 kN/m that was input to the program. The fixities at the boundaries allow deformations in vertical direction (roller hinge in y-direction). Unit weights of the backfill and of the foundation soil are 17.3 and 18.2 kN/m^3, respectively, based on the laboratory results.

Each analysis was carried out by increasing the gravitational acceleration at a very small load increment to reach the point where no convergence was acquired. Then, the analyses continued with steps back by oscillating back and forth around the smaller increments to ensure convergence with an accuracy of 0.0001g. A large number of iterations was applied based on the fictitious viscoplasticity algorithm (Zienkiewicz et al., 1975; Kobayashi, 1984 and 1988; Zienkiewicz and Taylor, 1990) to calculate the load and consequently the collapse height of the slopes. During the analysis the vertical deformation of the crest is measured, as the gravitational acceleration increases (see Figure 4).

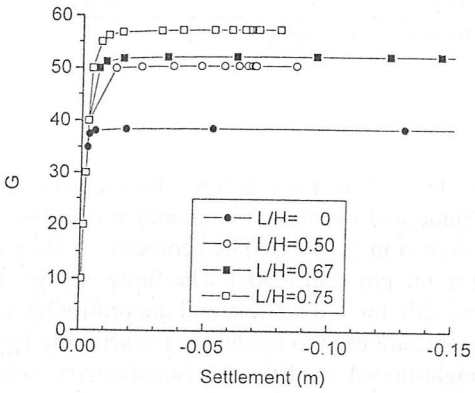

Fig. 4 Gravitational acceleration versus crest settlement

4.0 DISUSSION OF RESULTS

Table 2 presents the results of physical and numerical modeling of different vertical walls in terms of centrifugal accelerations and prototype equivalent heights. The characterization of tension crack is not possible during the analysis due to material discontinuity which results from cracking. However, the centrifugal acceleration at the time when tension crack occurs is approximately estimated from the load-settlement curves for each model. The criterion is to determine the gravitational acceleration at which the initial tangent in the elastic region intersects the tangent to the curve at a small deformation resulting from development of tension crack. The failure, however, is clearly defined when large deformation occurs at constant stress levels, as shown in Figure 4.

Table 2. Comparison of centrifugal accelerations and prototype heights

Model No.	$(N_c)_{EXP}$	$(N_f)_{EXP}$	$(N_c)_{FEM}$	$(N_f)_{FEM}$	$(H_c)_{EXP}$	$(H_f)_{EXP}$	$(H_c)_{FEM}$	$(H_f)_{FEM}$
M-34	34	35	37	38.7	5.17	5.32	5.62	5.88
M-48	34	40	40	50.6	5.17	6.08	6.08	7.69
M-49	36	49	40	52.5	5.47	7.45	6.08	7.98
M-28	40	54	50	57.5	6.08	8.21	7.60	8.74

$(N_c)_{EXP}$=gravitational acceleration at tension crack obtained from centrifuge tests
$(N_f)_{EXP}$=gravitational acceleration at failure obtained from centrifuge tests
$(N_c)_{FEM}$=estimated gravitational acceleration at tension crack obtained from FEM analyses
$(N_c)_{FEM}$=gravitational acceleration at failure obtained from FEM analyses
$(H_c)_{EXP}$= prototype equivalent height at tension crack obtained from centrifuge tests
$(H_f)_{EXP}$= prototype equivalent height at failure obtained from centrifuge tests
$(H_c)_{FEM}$= estimated prototype equivalent height at tension crack obtained from FEM analyses
$(H_c)_{FEM}$= prototype equivalent height at failure obtained from FEM analyses

4.1 Prototype Equivalent Height

In a broad perspective, for vertical walls, the centrifugal accelerations and prototype equivalent heights from the analysis slightly overpredicts those from centrifuge tests, as shown in Table 2. In terms of gravitational acceleration at tension crack the prediction by this approximate technique is within 12 to 25% of the experimental values. In terms of gravitational acceleration at failure, which represents the collapse prototype equivalent height, the best prediction is for the reinforced model (M-28). The relative difference in this case is 3.5 g that accounts for the prototype equivalent height of 0.53 m, which is practically not much significant. However, the predicted failure accelerations are higher for walls with shorter reinforcements (i.e., M-48 and M-49), which is attributed to the type of failure.

4.2 Position of Slip Surfaces

The contours of maximum shear strains and yield zones with plastic deformations after failure are shown in Figure 5 for both unreinforced and reinforced walls. The traces of slip surfaces obtained from centrifuge model tests are also plotted in those Figures.

In the case of unreinforced model (M-34) the slip surface coincides with the peaks of shear strain contours at the bottom of the wall and slightly diverges as the crest. For the case of models with short reinforcements (M-48, M-49), the slip surfaces from physical tests are behind the contours of yield zones. This is not surprising when the failure characteristics of these models are taken into consideration. Experimental evidences based on the post-test observations revealed that the failure surfaces of these models occurred either far beyond the back of the reinforcement, as in model M-48, or it occurred just behind the reinforced zone, as in the case of M-49. Unlike model M-28 in which the failure was entirely internal, in both these cases the slip surfaces occurred outside the reinforced zone. One source of discrepancy with the numerical prediction may also be attributed to the initial state of the stresses in the model which was not modeled in this study due to the complexities in stress path during model construction and the partially saturated soil of the backfill.

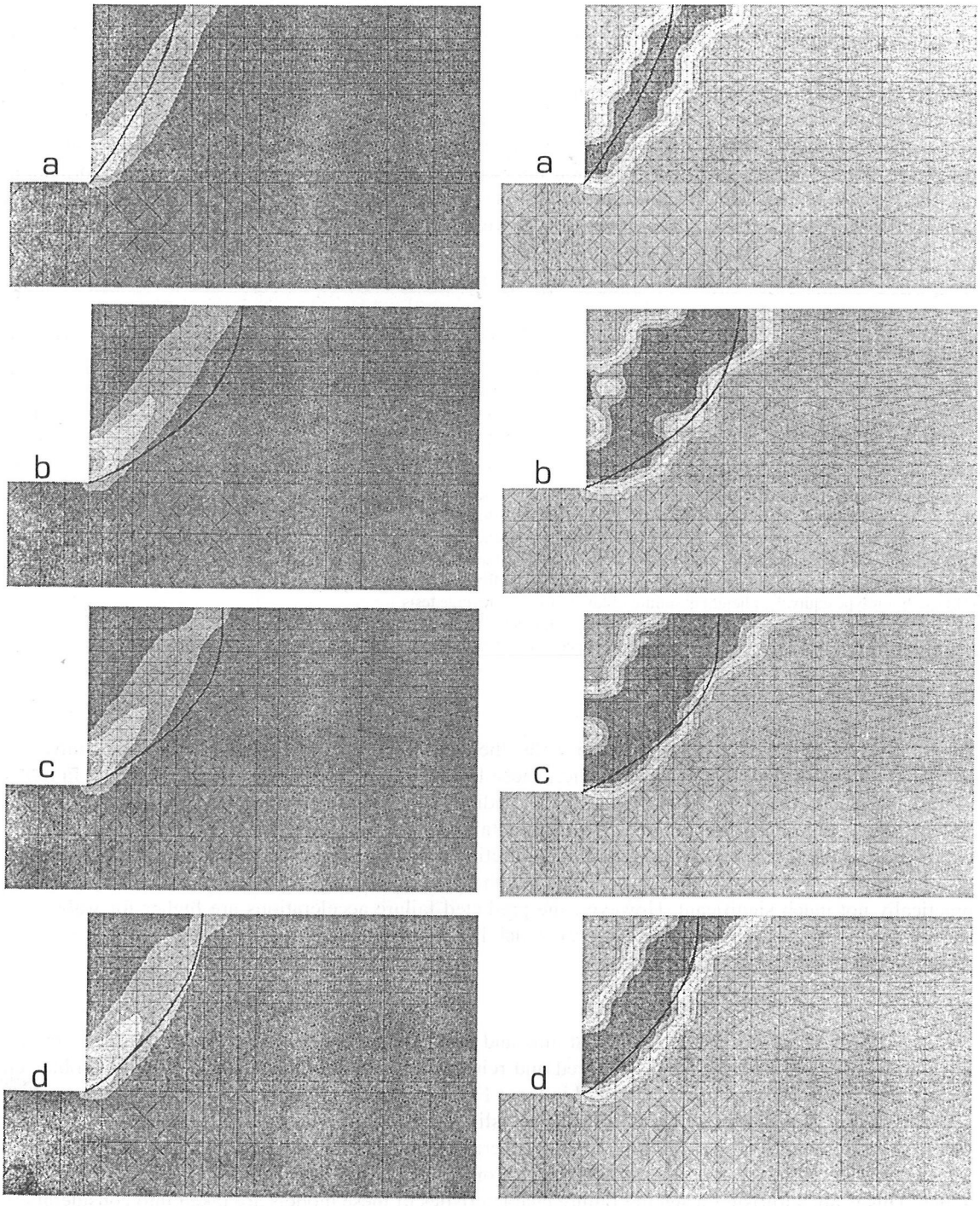

Fig. 5 Contours of maximum shear strain (left) and yield zones (right) for model walls: (a) M-34, (b) M-48, (c) M-49, and (d) M-28

In general, for the unreinforced model and the case of reinforced model (M-28) in which the failure surface is contained within the reinforced zone, the prediction of slip surfaces are reasonable. The slip

surfaces from physical modeling are located within these yield zones, even though the identification of clear-cut slip surface at the crest of the unreinforced wall is not as explicit as the body of the wall.

4.3 Deformed Mesh

The deformed meshes for both unreinforced and reinforced cases are shown in Figure 6. The deformed mesh at the toe for the case of unreinforced model will be improved as a result of selecting a finer mesh size.

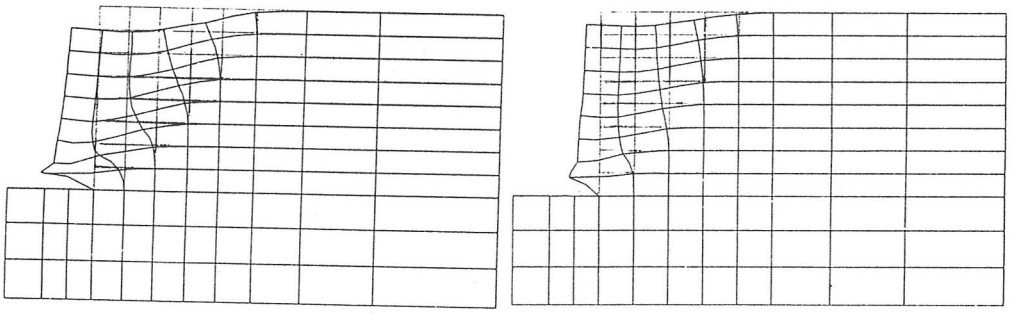

Fig.6: Deformed meshes for unreinforced and reinforced models

5. CONCLUSIONS

Understanding the behavior of reinforced retaining walls through experimental and numerical techniques is the subject of this study. The results of numerical simulation are presented to predict the behavior of geotextile reinforced walls with different reinforcement lengths that failed under self-weight in a geotechnical centrifuge. The eight-noded solid elements with elasto-plastic material properties and Mohr-Coulomb failure criterion is adopted to model the backfill and the foundation. The reinforcements are modeled by bar elements without flexural rigidities. The results of numerical simulation are compared with physical models and discussed in terms of tension crack development, gravitational acceleration and prototype equivalent height at failure. In general, the simulation is more successful to predict the behavior of the unreinforced case and the case of reinforced wall with L/H=0.75 in which failure is internal, i.e., the slip surface contains in the reinforced zone. The results show some deviations for the case where the failure is external. Overall, the numerical simulation slightly overpredicts the behavior of physical models in terms of prototype equivalent heights.

REFERENCES

1. Almeida, M.S.S., Britto, A.M., and Parry, R.H.G. (1986). Numerical modeling of a centrifuged embankment on soft clay, *Canadian Geotechnical Journal*, 23: 103-114.
2. Bolton, M.D., Sun, H.W., and Britto, A.M. (1993). Finite element analyses of bridge abutments on firm clay, *Computers and Geotechnics*, 15: 221-245.
3. Kobayashi, M. (1984). Stability analysis of geotechnical structures by finite elements, *Report of Port and Harbour Research Institute*, Vol. 23, No.1: 83-110.
4. Kobayashi, M. (1988). Stability analysis of geotechnical structures by adaptive finite element procedure, *Report of Port and Harbour Research Institute*, Vol. 27, No.2, June: 3-22.
5. Mitchell, J. K., and Villet, W. C. B. (1987). Reinforcement of earth slopes and embankments, NCHRP Report 290, Transportation Research Board, Washington D.C., 323.
6. Porbaha, A. and Goodings, D.J. (1996). Centrifuge modeling of geotextile reinforced walls, *Journal of Geotechnical Eng.*, ASCE, Vol.122, No.10,October 1996.
7. Porbaha, A., and Kobayashi, M., (1997). Finite element analysis of centrifuge model tests, submitted to the 6th International Symposium on Numerical Models in Geomechanics.

8. Row, R.K., and Soderman, K.L. (1985). An approximate method for estimating the stability of geotextile reinforced embankments, *Canadian Geotechnical Journal*, 22, No.3: 392-398.
9. Wu, T.H.J., Christopher, B. Siel, D., Nelson, N.S., Chou, H., and Helwany, B. (1992). The effectiveness of geosynthetic reinforced embankments constructed over weak foundation, *Geotextiles and Geomembranes*, 11: 133-150.
10. Zienkiewicz, O.C., and Humpheson, C., and Lewis, R.W. (1975). Associated and non-associated viscoplasticity and plasticity in soil mechanics, Geotechnique, Vol. 25: 671-689.
11. Zienkiewicz, O.C., and Taylor, R.L. (1990). The finite element method, McGraw Hill, fourth edition, Vol.2: 256-260.